Block of Current through Single Calcium Channels by Fe, Co, and Ni

Location of the Transition Metal Binding Site in the Pore

BRUCE D. WINEGAR, RONAN KELLY, and Jeffry B. Lansman

From the Department of Pharmacology, School of Medicine, University of California, San Francisco, California 94143-0450

ABSTRACT The blocking actions of Fe^{2+}, Co^{2+}, and Ni^{2+} on unitary currents carried by Ba^{2+} through single dihydropyridine-sensitive Ca^{2+} channels were recorded from cell-attached patches on myotubes from the mouse C2 cell line. Adding millimolar concentrations of blocker to patch electrodes containing 110 mM $BaCl_2$ produced discrete excursions to the closed channel level. The kinetics of blocking and unblocking were well described with a simple model of open channel block. Hyperpolarization speeded the exit of all of the blockers from the channel, as expected if the blocking site resides within the pore. The block by Ni^{2+} differs from that produced by Fe^{2+} and Co^{2+} because Ni^{2+} enters the channel ~20 times more slowly and exits ~50 times more slowly. Ni^{2+} also differs from the other transition metals because at millimolar concentrations it reduces the amplitude of the unitary current in a concentration-dependent manner. The results are consistent with the idea that the rate-limiting step for ion entry into the channel is water loss at its inner coordination sphere; unblocking, on the other hand, cannot be explained in terms of simple coulombic interactions arising from differences in ion size.

INTRODUCTION

Cations of the transition metal series bind to specific sites on proteins and are important in the catalytic activity of many enzymes. Although these ions generally bind at sites distinct from the Ca^{2+} binding sites of proteins, they share the common feature of blocking voltage-gated Ca^{2+} currents (reviewed in Hagiwara and Byerly, 1981; Edwards, 1982). The transition metals have been used extensively to block voltage-gated Ca^{2+} currents in a variety of cells and, in some instances, to separate individual components of Ca^{2+} channel current (reviewed in Bean, 1989). While it has been assumed these ions block current flow by binding to a site within the channel,

Address reprint requests to Dr. J. B. Lansman, Department of Pharmacology, School of Medicine, University of California, San Francisco, CA 94143-0450.

Dr. Kelly's present address is University Laboratory of Physiology, South Parks Road, Oxford, UK.

J. GEN. PHYSIOL. © The Rockefeller University Press · 0022-1295/91/02/0351/17 $2.00 351
Volume 97 February 1991 351–367

there is little direct information on the mechanism by which these ions inhibit the flow of permeant ions.

The present study was undertaken with this goal in mind. We investigated the block of Ba^{2+} currents through single dihydropyridine-sensitive Ca^{2+} channels in mouse myotubes by the group VIII transition metal ions Fe^{2+}, Co^{2+}, and Ni^{2+}. The results show that, when observed at the single-channel level, the block produced by Fe^{2+} and Co^{2+} differed fundamentally from that produced by Ni^{2+} even though their steady-state affinities for the channel fall within a similar range. The results are discussed in terms of the physical properties of these ions that determine the rates of blocking and unblocking and possible structural features of the pore revealed by the blocking kinetics.

A preliminary report of this work has been published as an abstract (Winegar et al., 1990).

METHODS

The methods for culturing myotubes from C2 cells have been described in detail previously (Lansman, 1990; Winegar and Lansman, 1990). In these experiments, we used the dihydropyridine agonist (+)−202−791 (Sandoz Ltd., Basel, Switzerland) to increase the duration of the single-channel openings so that blocking transitions could be easily detected. Strong depolarizing prepulses to ~ +50 mV were applied to cell-attached patches to activate channels. Unitary events were detected after repolarizing the membrane to the test potential (Lansman, 1990). The records shown do not include the current during the prepulse and represent segments of channel activity measured at the indicated test potentials.

Solutions

The patch electrode filling solution contained 110 mM $BaCl_2$, 10 mM glucose, and 10 mM HEPES. The pH was adjusted to 7.5 by adding tetraethylammonium hydroxide (TEA-OH). Fe, Co, or Ni (>99.9% purity; Aldrich Chemical Co., Milwaukee, WI) was added to the electrode filling solution directly as the chloride salt. Hydrolysis of Co^{2+} and Ni^{2+} is negligible at pH 7.5 and the divalent ion is the predominant species in solution (Smith and Martell, 1976). Adding the chloride salt of Fe^{2+} to the pipette solution produced precipitates of polymeric oxides and hydroxides (Burgess, 1978). The pH of solutions containing Fe^{2+} was adjusted to pH 6.5 to prevent the formation of these insoluble products. Because of the difficulty associated with controlling the concentration of free Fe^{2+} in these experiments, we did not investigate the dependence of its blocking actions on its concentration. The data for Fe^{2+} are presented only to illustrate qualitative trends.

The bathing solution contained 150 mM K-aspartate, 5 mM $MgCl_2$, 10 mM K-EGTA, and 10 mM HEPES, and the pH was adjusted to 7.5 with TEA-OH. The isotonic K^+ solution was used to zero the cell's resting potential (Hess et al., 1986). Measuring the single-channel current–voltage (*I-V*) relation before and after exercising the patch from the membrane indicated the patch potential could be in error by ~ 10 mV.

Analysis of the Duration of Discrete Open and Blocked Lifetimes

Fe^{2+} and Co^{2+} produced blocking events that were just detectable at 0 mV. Because the closures were so brief relative to the 2-kHz bandwidth of the recording system, many of the blockages would not have been detected with the half-threshold crossing detection method used to measure the lifetime of the open and blocked states. We corrected the open times for missed

blockages following the general approach outlined by Colquhoun and Sigworth (1983) and Blatz and Magleby (1986) under the assumption that only blocking events were missed. Making this assumption would not produce a large error in estimating open times because fewer than ~10% of the openings were missed in most of the experiments. The correction procedure assumes that an exponential fit to the distribution of blocked times provides an accurate estimate of the blocked time constant.

Undetected blocking events would cause the mean open time obtained from the exponential fit to the open time histogram to be larger than the true open time because individual openings separated by a missed blocked period would be detected as a single event. In these experiments, ~60% of the blocking events produced by Co^{2+} and ~70% of the blocking events produced by Fe^{2+} escaped detection at 0 mV. The ratio of the number of missed blockages to the total number of blockages was calculated as

$$1 - \exp(-D/\mu_c) \quad (1)$$

where D is the dead time of the recording system (200 μs) and μ_c is the mean closed time obtained from the exponential fit. Mean open times obtained from the time constant of the exponential fit to the lifetime histograms were corrected by multiplying the uncorrected mean open time by the ratio of the detected to the total number of blocking events and then subtracting the sum of the duration of all missed closings. The sum of the duration of all missed closings was obtained by multiplying the number of missed events by the dead time.

The correction for missed blockages was tested by simulating single-channel data using the transition rates taken from the analysis of real records. These rates were used to specify a two-state stochastic process and Gaussian noise was added to the simulated records. The records of simulated channel activity were filtered at one-fifth the sampling rate and were then analyzed with the half-threshold method to obtain open and closed times. The corrected transition rates were within 10% of the rates specified for the simulation.

Analysis of Amplitude Distributions

At high blocker concentrations or at very negative membrane potentials the blocking and unblocking rates became very fast (Figs. 2 and 7). To obtain the rate constants for blocking and unblocking we analyzed the distribution of current amplitudes by fitting a beta function to the data (FitzHugh, 1983; Yellen, 1984). The amplitude distribution of the open channel current was measured and compared with the theoretical beta function obtained by specifying the transition rates and the filter cut-off frequency. The numerically generated beta function was convolved with a Gaussian function obtained from a fit to the closed channel noise and the transition rates changed to obtain the best fit by eye. Experiments with low concentrations of Fe^{2+} and Co^{2+} were refiltered with a lower cut-off frequency so that the slower blocking kinetics would be in a range, relative to the system bandwidth, where the single-pole filter approximation used to derive the beta distribution would be valid (Yellen, 1984). Blocking and unblocking rates obtained from amplitude distribution analysis were pooled with those obtained from measurements of the lifetime of open and blocked states.

Spectral Analysis

Power density spectra of open channel current fluctuations were measured in the presence of different concentrations of Fe^{2+} or Co^{2+}. The power spectrum of the closed channel noise in each experiment was subtracted from that of the open channel current. The subtracted spectra were fit with a single Lorentzian function. We found, however, that the corner frequency was independent of the concentration of blocker. For a simple transition between an open and a blocked channel the Lorentzian should have a single time constant (Neher and Steinbach,

1976; Ogden and Colquhoun, 1985):

$$\tau = 1/2\pi f_c \tag{2}$$

where f_c is the corner frequency. The reciprocal of the time constant is the sum of the blocking and unblocking rates. The relation between $2\pi f_c$ and the transition rates for a two-state blocking reaction is

$$2\pi f_c = k_{off} + k_{on}[B] \tag{3}$$

where k_{off} is the unblocking rate and $k_{on}[B]$ is the product of the blocking rate and the blocking ion concentration. When $k_{off} >> k_{on}[B]$, $2\pi f_c$ will be dominated by the unblocking rate and will therefore be independent of the concentration of blocking ion in the electrode. We did not correct for filtered variance in the net power spectra because the known (filtered) variance was very close to estimates of the variance of the unfiltered signal (Ogden and Colquhoun, 1985).

RESULTS

Fig. 1 shows examples of single-channel records in which the electrode contained 110 mM $BaCl_2$ (top) or 110 mM $BaCl_2$ with either 0.5 mM Fe^{2+}, 0.5 mM Co^{2+}, or 2 mM Ni^{2+}. The unitary currents were recorded at 0 mV after a strong depolarizing

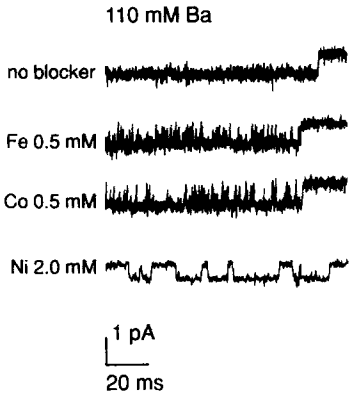

FIGURE 1. Block of unitary Ba^{2+} current by Fe^{2+}, Co^{2+}, and Ni^{2+}. The patch electrode contained 110 mM $BaCl_2$ and the indicated concentration of blocking ion. Unitary currents were recorded at 0 mV after a strong depolarizing prepulse (+30 to +50 mV).

prepulse that was used to activate channels (details of the experimental procedure are described in Lansman, 1990). The records show that adding Fe^{2+} or Co^{2+} to the patch electrode produced very brief interuptions in the open channel current that were just detectable at the 2-kHz recording bandwidth, while the blockages produced by Ni^{2+} were greater than two orders of magnitude longer in duration and well resolved even at the 1-kHz filter cut-off frequency used in the experiment shown in the figure. The records also show that Fe^{2+} and Co^{2+} produced many more blockages than did Ni^{2+} at a fourfold lower concentration. The experiments that are described below analyzed the kinetics of channel blockade produced by each of these ions.

Block of Ba^{2+} Currents by Fe^{2+} and Co^{2+}

We first analyzed channel block by Co^{2+} to see if the rapid transitions to the closed channel level arose from the entry of blocking ion into the open channel. The

transitions of the single-channel current between the open and closed channel levels were analyzed with the help of a simple two-state model for open channel block which has been used previously to analyze the block of unitary Ca^{2+} channel currents by other multivalent cations (Lansman et al., 1986; Lansman, 1990; Winegar and Lansman, 1990).

The records in Fig. 2 are from three separate experiments in which the patch electrode contained either 0.5, 1, or 2 mM Co^{2+}. Fig. 2 shows that increasing the concentration of Co^{2+} in the electrode increased the frequency of blocking events. At the higher concentrations of Co^{2+}, the transitions to the closed (blocked) state appeared to be more frequent and, at the highest concentrations, difficult to resolve as discrete closings, which gave the appearance of rapid, flickery block.

The kinetics of channel block were analyzed by measuring the durations of the open and blocked times within a burst of openings. Bursts were identified as a series of rapid openings and closings in the single-channel record. Bursts are easy to identify in the records of Ca^{2+} channel openings in C2 myotubes because the

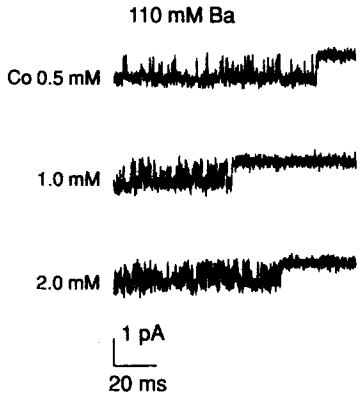

FIGURE 2. Block of unitary Ba^{2+} currents by Co^{2+}. Currents were recorded at 0 mV from three different patches in which the pipette contained 110 mM Ba^{2+} and either 0.5, 1, or 2 mM Co^{2+}.

presence of dihydropyridine agonist prolongs channel openings and there are virtually no fast gating transitions in the single-channel record. Under these conditions virtually all of the closings can be attributed to blocking events (Lansman, 1990).

The histograms of open and blocked times measured in experiments in which the electrode contained either 0.5 or 1 mM Co^{2+} are shown in Fig. 3. The smooth curve drawn through each histogram represents the maximum likelihood exponential fit to the data with the indicated time constant. The histograms were well fit with a single exponential, suggesting the existence of a single open and a single blocked state. The mean open time decreased from 1.7 ms with 0.5 mM Co^{2+} in the electrode to 0.8 ms with 1 mM Co^{2+}. The mean blocked times, however, remained relatively unchanged when the concentration of Co^{2+} in the electrode was increased.

With higher concentrations of Co^{2+} in the electrode where it was difficult to discern discrete blocking and unblocking events, the kinetics of block were analyzed by fitting a theoretical beta distribution to the amplitude histogram of the open channel

current as described in the Methods (see also Yellen, 1984; Winegar and Lansman, 1990). Fig. 4 *A* shows examples of the amplitude distributions of the open channel current at 0 mV in the presence of either 1 or 2 mM Co^{2+} in the electrode. The fit of a beta distribution to the data is indicated by the smooth curve superimposed on the experimental points. The transition rates used to generate the beta distribution that was fit to the amplitude distribution were similar to those obtained from an analysis of the lifetimes of the open and blocked states.

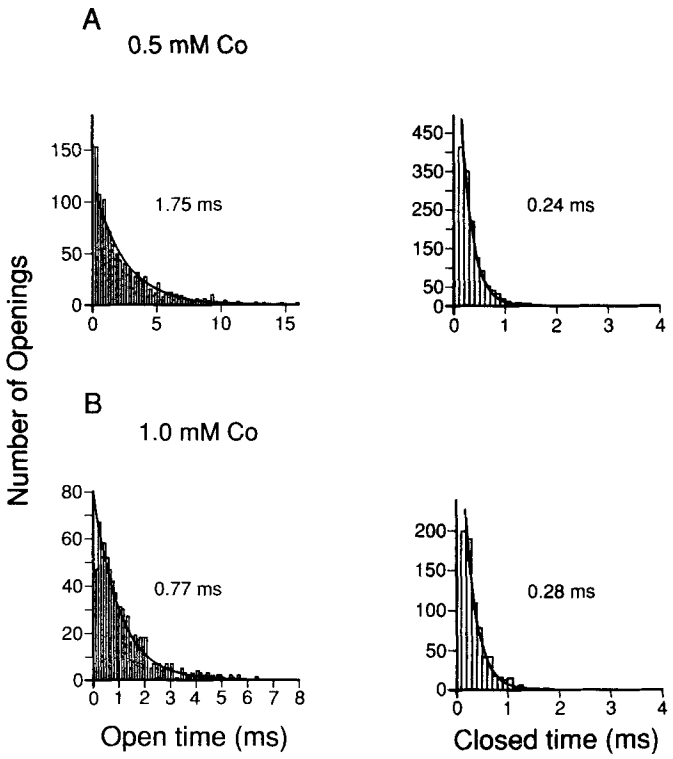

FIGURE 3. Concentration dependence of the kinetics of the block of unitary Ba^{2+} currents by Co^{2+}. Histograms of open and blocked times measured from two experiments in which the patch electrode contained either 0.5 mM (*top*) or 1 mM Co^{2+} (*bottom*). The smooth curves through the histograms represent the maximum likelihood fit to a single exponential with the indicated time constant.

As an additional test of the accuracy of the measurements of the blocking kinetics, we analyzed the power density spectra for the fluctuations of the open channel current as shown in Fig. 4 *B*. We found that the power density spectra were well fit by a single Lorentzian function as expected for a simple two-state process. The corner frequency, however, was relatively independent of the concentration of blocker (Fig. 4, *A* and *B*, right panels), suggesting that unblocking was much faster than blocking (see Methods). In support of this interpretation, the values of the reciprocal of the

time constant from the single Lorentzian fit were close to the unblocking rates obtained by measuring the mean blocked time as well as from amplitude distribution analysis. The results suggest that the single Lorentzian process observed in the power density spectra corresponds to the two-state blocking process in which the time constant reflects primarily the rate of unblocking.

To test the predictions of the open channel block model, the inverse of the blocking and unblocking rates were plotted as a function of the concentration of Co^{2+}

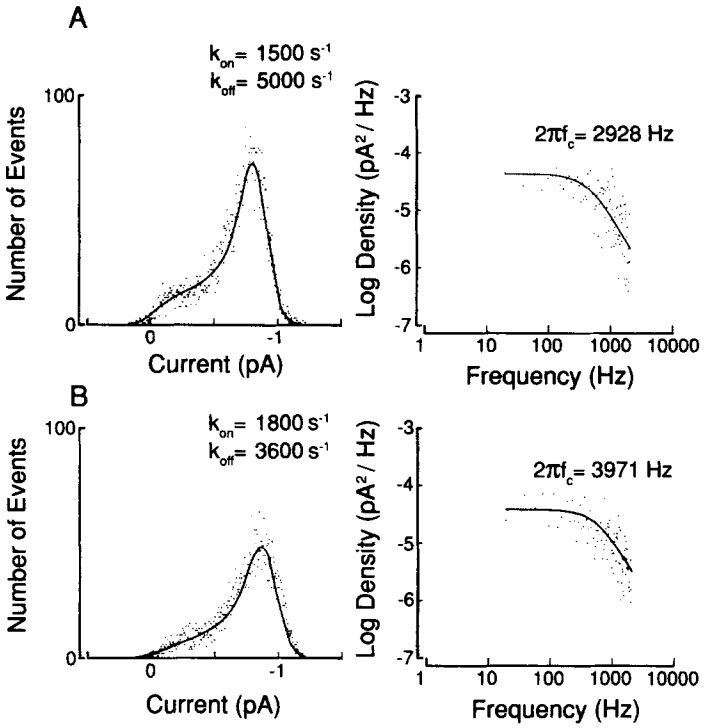

FIGURE 4. Analysis of the Co^{2+} blocking kinetics from the distribution of current amplitudes and power density spectra. (*A*) An experiment with 1 mM Co^{2+} in the electrode. The amplitude distributions were fit to a beta function (*solid line*) with the indicated rate constants. The power density spectrum on the right was obtained after subtracting the closed channel noise and was fit to a single Lorentzian function with the indicated corner frequency ($2\pi f_c$). (*B*) Analysis of the blocking kinetics obtained as in *A* in an experiment in which the patch electrode contained 2 mM Co^{2+}.

in the electrode as shown in Fig. 5. Measurements of the mean lifetimes of the open (after correction for missed events as described in the Methods) and blocked times are shown with filled symbols, while the rates obtained from fitting a beta function to the amplitude distribution are shown with open symbols. Fig. 5, *A* and *B*, shows that the kinetic constants obtained by each of the methods agree within experimental error. The slope of the relation between blocking rate and the concentration of Co^{2+} in the electrode gave a second-order rate coefficient of $k_{on} = \sim 8.7 \times 10^5\ M^{-1}s^{-1}$.

Increasing the concentration of Co^{2+} in the electrode, on the other hand, did not change the rate of unblocking in any consistent manner. The mean blocked time at 0 mV was obtained by averaging all the measurements and was $\sim$4,300 s^{-1}.

Because of the difficulties of controlling the concentration of free Fe^{2+} in solution at physiological pH (see Methods), we analyzed only the blocked times in the presence of a fixed concentration. Nevertheless, the measurements provide information on the rate of unblocking, which can be used to compare Fe^{2+} with other transition metal blockers. Fig. 6 (*top*) shows the unitary Ba^{2+} current recorded at 0 mV with 0.5 mM Fe^{2+} in the pipette and illustrates that, like Co^{2+}, Fe^{2+} produces rapid blockages in the single-channel record. As shown in Fig. 6 (*middle*), histograms

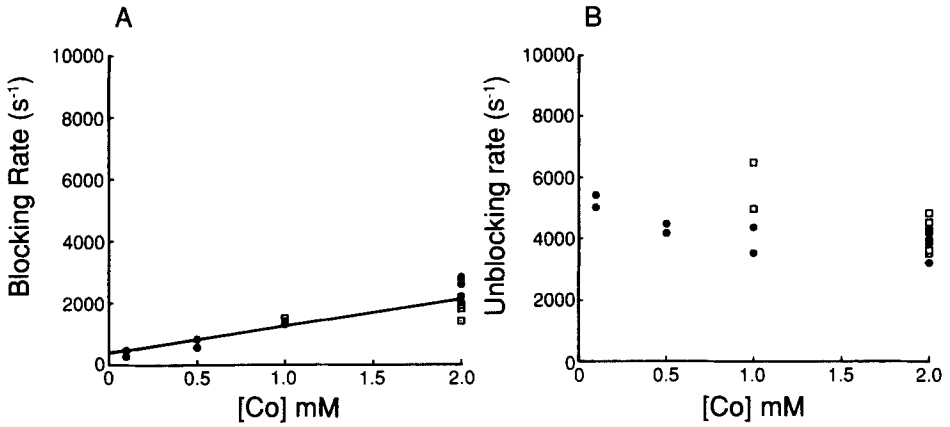

FIGURE 5. Concentration dependence of the blocking kinetics produced by Co^{2+}. (*A*) The inverse of the mean open time obtained from analysis of the lifetimes of the open and blocked states (*filled circles*) and blocking rate obtained from the fit of the amplitude distribution with a beta function (*open squares*). Each point represents data from a different patch. The patch potential was 0 mV. The straight line through the points is a least-squares fit with a slope of 8.7×10^5 $M^{-1}s^{-1}$, which is the second-order rate constant for Co^{2+} entry into the channel. (*B*) Dependence of the inverse of the mean blocked time on the concentration of Co^{2+}. Filled circles are the inverse of the mean blocked time; open squares are unblocking rates from amplitude distribution analysis. The mean unblocking rate from both measurements was $\sim$4,300 s^{-1}.

of open and blocked times were also well fit with single exponentials, as expected for a simple two-state blocking process. The unblocking rates also agreed well with measurements obtained from fitting a beta function to the distribution of current amplitudes (Fig. 6, *bottom left*) or from the corner frequency obtained from the fit of a single Lorentzian to the power density spectrum of the open channel current (Fig. 6, *bottom right*): the reciprocal of the mean blocked time was $\sim$7,100 s^{-1}; the unblocking rate obtained from amplitude distribution analysis was $\sim$6,500 s^{-1}; while the rate constant obtained from the corner frequency of the Lorentzian fit to the power spectrum of the open channel current was $\sim$5,100 s^{-1}. Although there is some

scatter in the measurements, the general agreement is good considering that different methods were used to obtain the rates of unblocking.

To obtain information on the location of the energy barriers to ion blocking and unblocking, we analyzed the voltage dependence of the block produced by Co^{2+}. Fig. 7 shows records from an experiment in which the electrode contained 0.5 mM Co^{2+}. The records shown in Fig. 7 were obtained after the patch potential was stepped to 0, −20, or −40 mV. The records show that as the patch potential was made more negative, the number of blocking events appeared to increase.

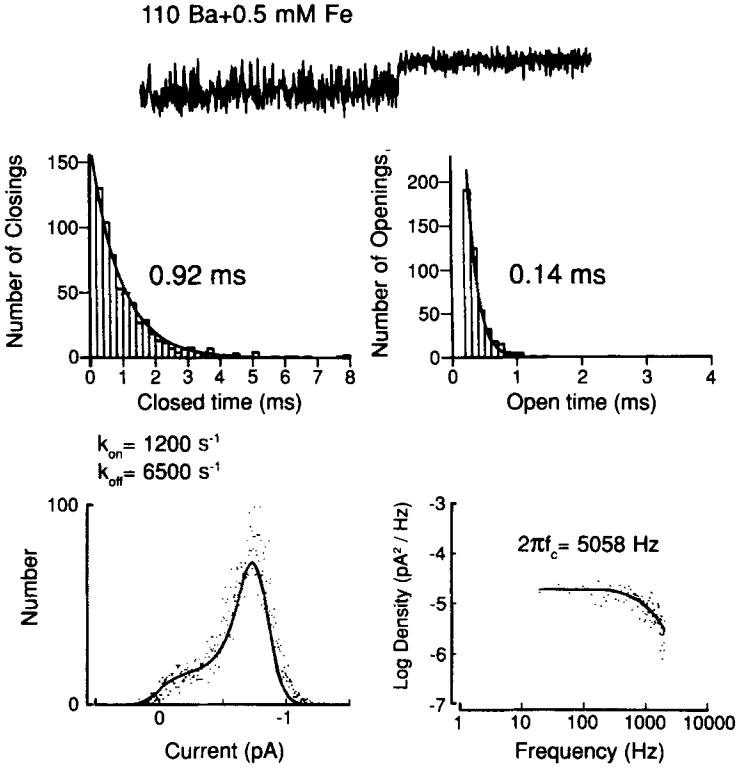

FIGURE 6. Analysis of the block of unitary Ba^{2+} current by 0.5 mM Fe^{2+}. At center, histograms of open (*left*) and blocked times (*right*). The smooth curve through the histograms represents the maximum likelihood fit to a single exponential with the indicated time constant. At bottom left, amplitude distribution from the same experiment with a fitted beta distribution with the indicated transition rates. At bottom right, power density spectra of the open channel current. The curve is a fitted single Lorentzian function with a corner frequency f_c = 805 Hz.

Fig. 8 shows the analysis of the voltage dependence of the block produced by Co^{2+} obtained from an analysis of records like those shown in Fig. 7. Fig. 8 *A* shows the voltage dependence of the blocking rate (filled symbols) and unblocking rate (open symbols) obtained from the analysis of lifetimes of the open and blocked states (triangles) and from an analysis of the distribution of current amplitudes (circles). The rates are plotted against the patch potential on a semilogarithmic scale. An

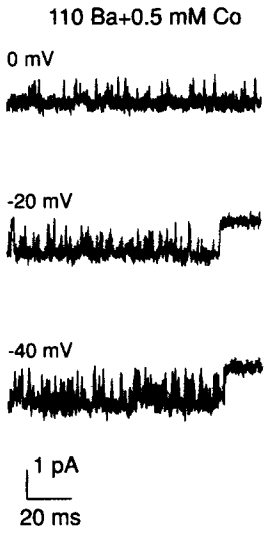

FIGURE 7. Voltage dependence of the block produced by 0.5 mM Co^{2+} in an experiment in which the patch potential was 0, −20, or −40 mV.

exponential fit to the data points showed that the unblocking rate increased ~*e*-fold per 90 mV, while the blocking rate increased ~*e*-fold per 130 mV.

To verify the voltage dependence of the unblocking kinetics, particularly at negative membrane potentials where the rate became too fast to detect blockages as discrete events, we analyzed the power spectra of the current fluctuations produced by Co^{2+}. Fig. 8 *B* shows the corner frequency obtained from the fit to a single Lorentzian for the current fluctuations produced by Co^{2+} at different patch poten-

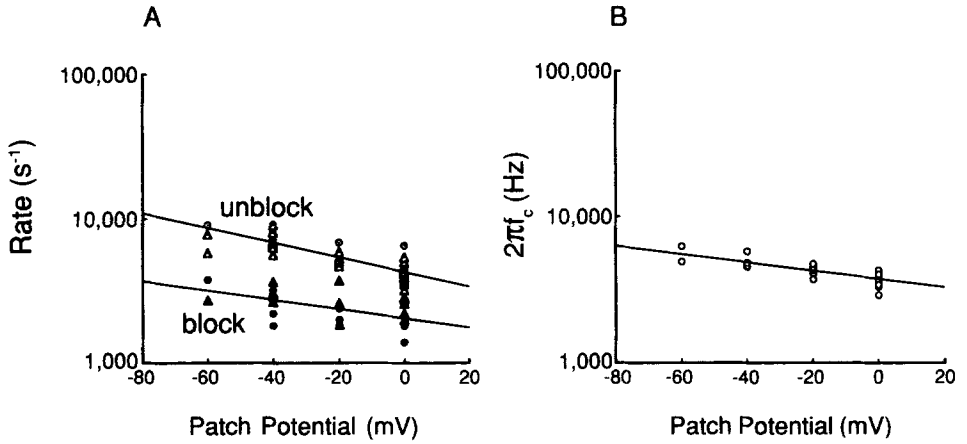

FIGURE 8. Kinetic analysis of the voltage dependence of the block of unitary Ba^{2+} currents by Co^{2+}. (*A*) The dependence on the patch potential of the inverse of the mean open time (*filled triangles*) or the blocking rate from amplitude distribution analysis (*filled circles*) and the inverse of the mean blocked time (*open triangles*) and the unblocking rate from amplitude distribution analysis (*open circles*). (*B*) The dependence on the patch potential of the corner frequency obtained from a fit of the power density spectra to a single Lorentzian ($2\pi f_c$).

tials. These values were somewhat smaller than those obtained by the other methods and the dependence on membrane potential was also less steep. However, the rate of unblocking increased as the patch potential was made more negative, consistent with the analysis shown in Fig. 8 *A*.

Block of Ba^{2+} Currents by Ni^{2+}

Block of unitary Ba^{2+} currents by Ni^{2+} differed in several ways from the block produced by Fe^{2+} and Co^{2+}. The blockages produced by Ni^{2+} lasted very long and could easily be detected in the single-channel records. Fig. 9 *A* shows records of

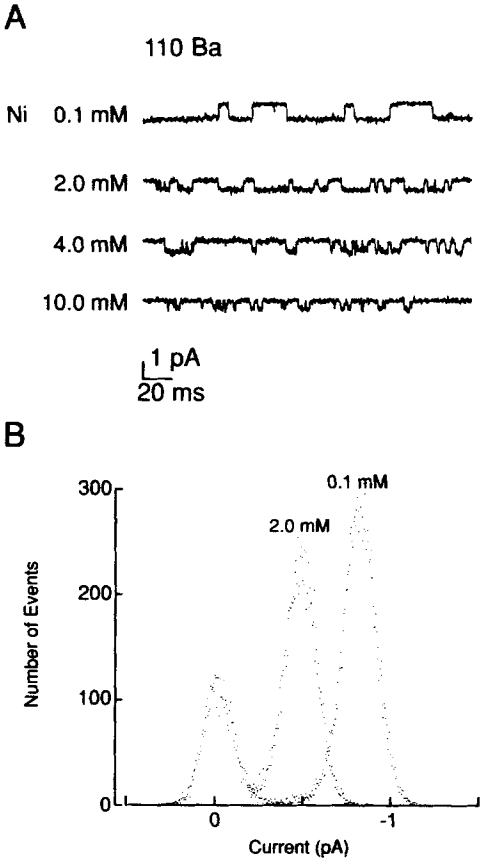

FIGURE 9. Block of unitary Ba^{2+} currents by Ni^{2+}. (*A*) Unitary Ba^{2+} currents recorded at 0 mV in the presence 0.1, 2, 4, and 10 mM Ni^{2+}. (*B*) Amplitude distribution of the open channel current in the presence of (*a*) 0.1 mM Ni^{2+} and (*b*) 2 mM Ni^{2+}. The amplitude of the unitary Ba^{2+} current in the presence of 0.1 mM Ni^{2+} was ~0.79 pA; the amplitude in the presence of 2 mM Ni^{2+} was ~0.47 pA.

channel activity at 0 mV in the presence of 110 mM $BaCl_2$ and the indicated concentration of Ni^{2+} in the patch electrode. Unlike Fe^{2+} and Co^{2+}, millimolar concentrations of Ni^{2+} reduced the amplitude of the unitary current. Fig. 9 *B* shows the distribution of current amplitudes in the presence of (*a*) 100 μM and (*b*) 2 mM Ni^{2+}. The amplitude of the unitary Ba^{2+} current was 0.79 pA in the presence of 100 μM Ni^{2+}, 0.55 ± 0.20 pA (mean ± SD, n = 5) in the presence of 2 mM Ni^{2+}, and 0.50 ± 0.05 pA (mean ± SD, n = 3) in the presence of 10 mM Ni^{2+}. In spite of the reduction of the unitary current, which appeared to saturate at concentrations of Ni^{2+}

greater than ~4 mM, discrete blockages could be observed in the single-channel records at all concentrations.

Fig. 10 *A* shows the analysis of the lifetimes of the open and blocked states at two concentrations of Ni^{2+} (2 and 10 mM). Open times were reduced by increasing the concentration of Ni^{2+} in the electrode, while the closed times remained constant. Fig. 10 *B* shows the inverse of the mean open and blocked times obtained from the single exponential fit plotted as a function of concentration. As predicted by the model for open channel block, the inverse of the mean open time depended linearly on blocker concentration, while the inverse of the mean blocked time was concentration independent. The slope of the relation between blocker concentration and the

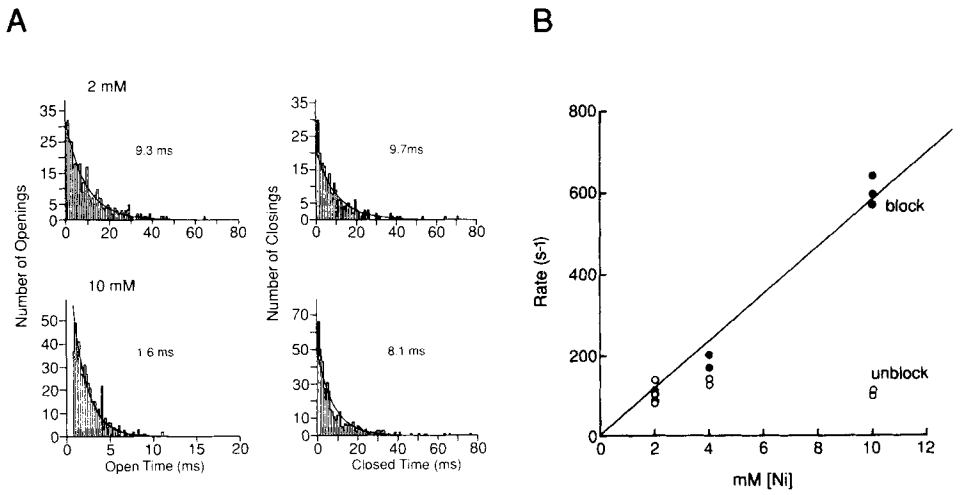

FIGURE 10. Kinetic analysis of the block of unitary Ba^{2+} currents by Ni^{2+}. (*A*) Histograms of open and blocked times from two experiments in which the patch electrode contained either 2 or 10 mM Ni^{2+}. The smooth curve through the histogram is the single exponential fit with the indicated time constant. (*B*) The inverse of the mean open times (*filled circles*) and blocked times (*open circles*) are plotted as a function of the concentration of Ni^{2+} in the electrode. The second-order rate coefficient for Ni^{2+} obtained from the least-squares fit of the concentration dependence of the inverse of the blocking rate was $\sim 6.0 \times 10^4$ $M^{-1}s^{-1}$. The fit was constrained to pass through zero.

inverse of the mean open time gives a second-order blocking rate coefficient of $\sim 6.0 \times 10^4$ $M^{-1}s^{-1}$. The unblocking rate was ~100 s^{-1}. Evidently, Ni^{2+} enters the channel ~20 times more slowly and exits the channel ~50 times more slowly than Co^{2+}.

Fig. 11 *A* shows records of the blocking actions of 2 mM Ni^{2+} in a single experiment in which the patch potential was 0, −20, and −40 mV. Hyperpolarizing the patch potential appeared to shorten the blocking events. The kinetics of blocking and unblocking were analyzed at different patch potentials and the results were plotted as a function of the patch potential on a semilogarithmic scale in Fig. 11 *B*. A fit to the data showed the blocking rate increased ~*e*-fold per 55 mV of hyperpolar-

ization, while the unblocking rate increased ~e-fold with 33 mV hyperpolarization. The results show that the rate of unblocking increases more steeply with membrane potential than does the rate of blocking and this would reduce the extent of steady-state block at more negative potentials (cf. Winegar and Lansman, 1990).

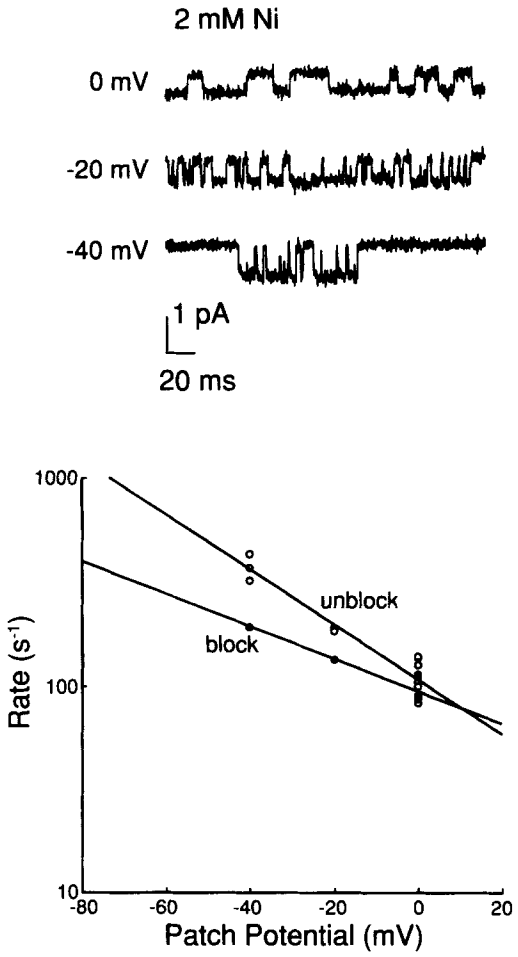

FIGURE 11. Voltage dependence of Ni^{2+} block of unitary Ba^{2+} current. (*Top*) Unitary Ba^{2+} currents from a single patch with 2 mM Ni^{2+} in the electrode recorded at the indicated patch potentials. (*Bottom*) Inverse of the mean open times (*filled circles*) and closed times (*open circles*) plotted as a function of the patch potential on a semilogarithmic scale.

DISCUSSION

Relation to Previous Work

The transition metals are widely used as inhibitors of Ca^{2+} channel currents (reviewed in Hagiwara and Byerly, 1981; Edwards, 1982), however, there have been few studies that have measured the steady-state inhibitory constants for a series of blockers. Nachsen (1984) studied the block produced by a wide variety of multivalent cations on K^+-stimulated $^{45}Ca^{2+}$ uptake into rat brain synaptosomes and showed that Co^{2+}

and Ni^{2+} blocked Ca^{2+} uptake with roughly equal affinities (~50 μM). On the other hand, Narahashi et al. (1987) showed that Ni^{2+} and Co^{2+} block both a sustained and a transient component of macroscopic Ba^{2+} current in neuroblastoma; however, the affinity of Ni^{2+} is two times greater for the sustained component and three times greater for the transient component.

As pointed out by Nachsen (1984), the group VIII transition metals belong to a class of metal ion blockers that have a relatively moderate affinity for the Ca^{2+} channel when compared with very strong blockers, such as Cd^{2+} and the lanthanides, and weaker blockers, such as Mg^{2+}. The present study confirms the observations of the blocking actions of the group VIII transition metals and shows that they inhibit current through dihydropyridine-sensitive channels in skeletal muscle, producing half-inhibition at concentrations that are within a factor of two to three of each other. The fact that the absolute concentrations of blocker that were required to inhibit current were higher than those used in previous studies is probably the result of the much higher permeant ion concentration used in this study, which would make competition between permeant ion and blocker for a channel site more severe (Lansman et al., 1986).

The main new finding is that the kinetics of channel block produced by group VIII transition metals differ significantly when observed at the single-channel level. While Fe^{2+} and Co^{2+} produce rapid blockages in the single-channel records, Ni^{2+} produces much longer blocking events that are comparable to those produced by high affinity blockers such as Cd^{2+} and the lanthanides (Lansman et al., 1986; Lansman, 1990). The results show that, although the affinity of Fe^{2+}, Co^{2+}, and Ni^{2+} for the channel may appear to be similar at the macroscopic level, the individual rate constants that determine affinity differ significantly. Thus Ni^{2+} binds tightly to its channel site, but entry into the channel is slow enough to reduce the overall equilibrium binding affinity. This contrasts with high affinity blockers such as Cd^{2+} and the lanthanides, which have extremely rapid entry rates, and where steady-state affinity is determined solely by the rate of blocker exit from the channel (Lansman et al., 1986; Lansman, 1990).

Ni^{2+} also reduces the amplitude of the unitary Ba^{2+} current at concentrations exceeding ~1 mM. The reduction of the unitary current occurs in addition to the block of the open channel because increasing the concentration of Ni^{2+} shortens the mean channel open time at the same time it reduces of the amplitude of the unitary Ba^{2+} current (Fig. 9 *A*). A number of mechanisms could explain the reduction of the unitary current. These include a rapid, unresolved block of the open channel, perhaps involving a channel site distinct from that involved in the slower blocking process, or a conformational change in the channel protein induced by the binding of Ni^{2+}. Alternatively, depletion of the main charge carrier by binding to negative charges at the mouth of the channel could also reduce the current amplitude. It is unlikely that surface charge effects play a major part in the reduction of current amplitude (cf. Muller and Finkelstein, 1976) because most charges would be screened in the presence of 110 mM $BaCl_2$. Furthermore, 2 mM Co^{2+} did not reduce the unitary current, whereas 2 mM Ni^{2+} did. Although the experiments do not distinguish among these possible mechanisms, Ni^{2+} is, nonetheless, unique among the metal ions that block Ca^{2+} channels thus far studied at the single-channel level in producing discrete blockages and reducing the unitary current.

Mechanism of Block

The results show that hyperpolarization speeds the exit of all the blockers studied even though there are quantitative differences in the absolute values of the rate of unblocking. In having an unblocking rate that increases with hyperpolarization, the transition metals resemble other blockers studied at the single-channel level such as Cd^{2+}, Ca^{2+}, Zn^{2+}, and the lanthanides (Lansman et al., 1986; Lansman, 1990; Winegar and Lansman, 1990). The simplest interpretation is that the blocking site resides within the channel pore and the effect of hyperpolarization is to enhance the rate of blocker exit to the interior of the cell as predicted by a model of voltage-dependent channel block (Woodhull, 1973). The experiments leave open the question of the possibility of an interaction of permeant ions with blocker within the pore (cf. Lansman et al., 1986).

The physical factors governing blocker residence time within the channel are not completely understood. Electrostatic interactions arising from differences in ion size play an important part in determining divalent affinity for its channel binding site (Truesdell and Christ, 1967; Nachsen, 1984; Lansman, 1990). Yet the available data do not fit neatly within such a framework for the case of the transition metal ions which differ not only in size, but also in chemical properties such as polarizability and steric requirements of the coordination complex. The experimental results show that Ni^{2+}, which has an ionic radius of 0.55 Å (ionic radii from Shannon, 1976), resides within the channel some 50 times longer than Co^{2+} or Mg^{2+}, which have ionic radii of 0.58 and 0.57 Å, respectively, at a coordination number of four. The results point to the importance of noncoulombic forces in determining the residence time of transition metals within the pore.

Previous studies suggest that the rate-limiting step for ion entry into the Ca^{2+} channel depends primarily on the rate of water loss at the inner hydration sphere of the incoming ion (Lansman et al., 1986; Lansman, 1990). The results reported here extend the measurements of ion entry rates to Ni^{2+}, which has an exceptionally slow rate of dehydration. Ni^{2+} differs from other transition metal ions: it dehydrates ~100 times more slowly than Fe^{2+} and Co^{2+} and ~1,000 times more slowly than Zn^{2+} (Diebler et al., 1969). On the other hand, Ni^{2+} more closely resembles Mg^{2+}, although Ni^{2+} dehydrates about 10 times more slowly than Mg^{2+}. The results obtained from the analysis of the blocking kinetics agree well with the prediction that the rate of water loss at the incoming ion's inner coordination sphere determines its rate of entry into the channel. Thus Cd^{2+}, Ca^{2+}, Zn^{2+}, and the lanthanides have the fastest entry rates (~10^7–10^8 $M^{-1}s^{-1}$), Co^{2+} is somewhat slower (~10^6 $M^{-1}s^{-1}$), and Mg^{2+} and Ni^{2+} enter the channel with very slow rates (~2×10^5 and ~6×10^4 $M^{-1}s^{-1}$) in the presence of 110 mM Ba^{2+} at 0 mV (Lansman et al., 1986; Lansman, 1990; Winegar and Lansman, 1990), consistent with an Eigen-Diebler type mechanism for complex formation.

What Do the Blocking Kinetics Tell Us about the Structure of the Channel Pore?

Analysis of the block of monovalent currents through the Ca^{2+} channel in mouse lymphocytes by Fukushima and Hagiwara (1985) suggested that the Ca^{2+} complexation site is located ~60% of the voltage drop from the membrane surface. This is comparable to the block produced of unitary Ba^{2+} currents by the lanthanides, in

which the lanthanide complexation site appeared to be located between 40 and 70% of the potential drop from the membrane surface (Lansman, 1990). Because lanthanides substitute for Ca^{2+} at its binding site in proteins, it is likely that they bind at similar sites within the channel. On the other hand, analysis of the voltage dependence of the equilibrium blocking constant suggested that the group IIB metal Zn^{2+} binds to a site located ~15% from the membrane surface (Winegar and Lansman, 1990). Calculation of the effective electrical distances from the kinetic data indicates that Co^{2+} and Ni^{2+} bind ~6 and 20% of the potential drop from the membrane surface, respectively. The results are qualitatively consistent with the idea that, like Zn^{2+}, Co^{2+} and Ni^{2+} bind to a more superficial site within the pore than do Ca^{2+} or the lanthanides.

The nature of this transition metal site is of interest because it provides information on the structure of the channel near the external membrane surface. Transition metals prefer to bind to nitrogen donor groups (Martin, 1988), suggesting that the transition metal complexation site may be made up of a ring of nitrogens facing the interior of the pore. The site may resemble the cysteine-rich zinc finger-like sequences found in DNA binding proteins (Berg, 1986). Analysis of the lanthanide selectivity sequence, on the other hand, suggests the Ca^{2+} binding site is likely to possess one or two carboxylates and several carbonyl donor groups (Lansman, 1990). Because the amino acid sequence of Ca^{2+} binding sites in a wide variety of proteins is highly conserved, the site within the channel may resemble the E-F hands found in other Ca^{2+}-binding proteins (Strynadka and James, 1989). Recent sequence analysis of the α_1 subunit of the dihydropyridine-sensitive Ca^{2+} channel suggests that it possesses regions homologous to E-F hands (Babitch, 1990). Extension of such sequence analyses of the Ca^{2+} channel pore should tell whether a zinc finger points the way along the permeation pathway to a more deeply lodged E-F hand.

This work was supported by the National Institute of Health, the Muscular Dystrophy Foundation, and a Basil O'Connor Award from the March of Dimes Foundation.

Original version received 30 April 1990 and accepted version received 22 August 1990.

REFERENCES

Babitch, J. 1990. Channel hands. *Nature* 346:321–322.

Bean, B. P. 1989. Classes of calcium channels in vertebrate cells. *Annual Review of Physiology* 51:367–384.

Berg, J. 1986. Potential metal-binding domains in nucleic acid binding proteins. *Science* 232:485–487.

Blatz, A. L., and K. L. Magleby. 1986. Correcting single channel data for missed events. *Biophysical Journal* 49:967–980.

Burgess, J. 1978. Metal Ions in Solution. John Wiley & Sons, New York. 316–317.

Colquhoun, D., and F. J. Sigworth. 1983. Fitting and statistical analysis of single channel records. *In* Single-Channel Recording. B. Sakmann and E. Neher (eds.) Plenum Press, New York. 191–263.

Diebler, H. M., M. Eigen, G. Illgenfritz, G. Maas, and R. Winkler. 1969. Kinetics and mechanism of reactions of main group metal ions with biological carriers. *Pure and Applied Chemistry* 20:93–115.

Edwards, C. 1982. The selectivity of ion channels in nerve and muscle. *Neuroscience* 7:1335–1366.

FitzHugh, R. 1983. Statistical properties of the asymmetric random telegraph signal with applications to single-channel analysis. *Mathematical Bioscience* 64:75–89.

Fukushima, Y., and S. Hagiwara. 1985. Currents carried by monovalent cations through calcium channels in neoplastic B lymphocytes. *Journal of Physiology* 358:255–284.

Hagiwara, S., and L. Byerly. 1981. Calcium channel. *Annual Review of Neuroscience* 4:69–125.

Hess, P., J. B. Lansman, and R. W. Tsien. 1986. Calcium channel selectivity for divalent and monovalent cations. Voltage and concentration dependence of single channel current in ventricular heart cells. *Journal of General Physiology* 88:293–319.

Lansman, J. B. 1990. Blockade of current through single calcium channels by trivalent lanthanide cations. Effect of ionic radius on the rates of ion entry and exit. *Journal of General Physiology* 95:679–696.

Lansman, J. B., P. Hess, and R. W. Tsien. 1986. Blockade of current through single calcium channels by Cd^{2+}, Mg^{2+}, and Ca^{2+}. Voltage and concentration dependence of calcium entry into the pore. *Journal of General Physiology* 88:321–347.

Martin, R. B. 1988. Nickel ion binding to amino acids and peptides. *In* Metal Ions in Biological Systems. Vol. 23. Nickel and Its Role in Biology. H. Sigel (ed.) Marcel Dekker Inc., New York. 123–164.

Muller, R. V., and A. Finkelstein. 1974. The electrostatic basis of Mg^{2+} inhibition of transmitter release. *Proceedings of the National Academy of Sciences USA.* 71:923–926.

Nachsen, D. 1984. Selectivity of the Ca binding site in synaptosome Ca channels. *Journal of General Physiology.* 83:941–967.

Narahashi, T., A. Tsunoo, and M. Yoshii. 1987. Characterization of two types of calcium channels in mouse neuroblastoma cells. *Journal of Physiology* 383:231–249.

Neher, E., and J. H. Steinbach. 1976. Local anaesthetics transiently block currents through single acetylcholine-receptor channels. *Journal of Physiology* 277:153–176.

Ogden, D. C., and D. Colquhoun. 1985. Ion channel block by acetylcholine, carbachol, and suberyldicholine at the frog neuromuscular junction. *Proceedings of the Royal Society London B* 225:329–355.

Shannon, R. D. 1976. Revised effective ionic radii and systematic studies of interatomic distances in halides and chalcogenides. *Acta Crystallographica* A32:751–767.

Smith, R. M., and A. E. Martell. 1976. Critical Stability Constants. Vol. 4. Inorganic Complexes. Plenum Press, New York and London. 2–3.

Strynadka, N. C. J., and M. N. G. James. 1989. Crystal structures of the helix-loop-helix calcium-binding proteins. *Annual Review of Biochemistry* 58:951–998.

Truesdell, A. H., and C. L. Christ. 1967. Glass electrodes for calcium and other divalent cations. *In* Glass Electrodes for Hydrogen and other Cations. G. Eisenman, editor. Marcel Dekker, New York. 283–321.

Winegar, B., R. Kelly, and J. B. Lansman. 1990. Block of single calcium channels in C2 myotubes by Zn, Fe, Co, and Ni. *Biophysical Journal* 57:525*a*. (Abstr.)

Winegar, B., and J. B. Lansman. 1990. Voltage-dependent block by zinc of single calcium channels in mouse myotubes. *Journal of Physiology* 425:563–578.

Woodhull, A. 1973. Ionic blockage of sodium channels in nerve. *Journal of General Physiology* 61:687–708.

Yellen, G. 1984. Ionic permeation and blockade in Ca^{2+}-activated K^+ channels of bovine chromaffin cells. *Journal of General Physiology* 84:157–186.